



DRONE NORTH  
Drone Applications Specialists  
GEOMANTIA CONSULTING (Est. 2011)  
33 Roundel Rd, Whitehorse,  
YT, Canada, Y1A 3H4  
T: +1 867 335 5245  
E: geomantia@hotmail.com  
Venessa Bennett (Ph.D, P.Geo, Adv. Dip GIS/Remote Sensing)

# 2024 Report

## Describing

### LiDAR Reprocessing and Digital Mapping of the Nitra Project

**Location:** 63.842229°N, -135.633933°W

**Prepared For:** Banyan Corporation

**Prepared By:** Geomantia Consulting

**Report Date:** Jan 19, 2024

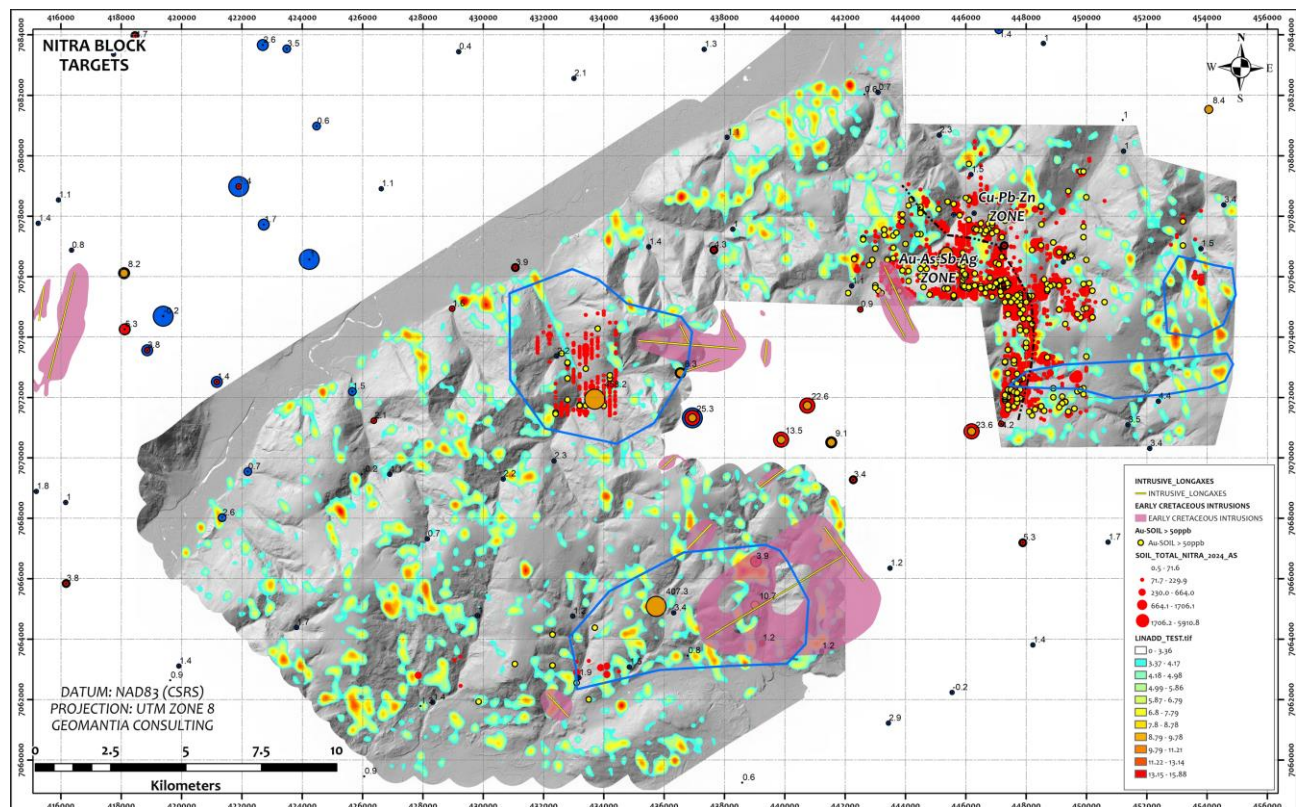


## **TABLE OF CONTENTS**

1.0 INTRODUCTION	4
2.0 REGIONAL TECTONIC SETTING	6
3.0 LiDAR REPROCESSING	8
4.0 LiDAR ANALYSIS PROCEDURES	12
5.0 LiDAR MAPPING RESULTS – NITRA PROPERTY	17
6.0 TARGETING	24
7.0 SUMMARY & RECOMMENDATIONS	30
8.0 STATEMENT OF QUALIFICATIONS	32

## LIST OF FIGURES

<b>FIGURE 1:</b> Location of Nitra project area, Banyan Gold Corp.	5
<b>FIGURE 2:</b> Regional geological setting of the Nitra Property, Banyan Gold Corp.	7
<b>FIGURE 3:</b> Simplified Early Cretaceous tectonic setting.	8
<b>FIGURE 4:</b> Comparison of 1 m vs 0.35 m resolution DTMs for Nitra project.	9
<b>FIGURE 5:</b> Hillshade models with 2 different sun illumination angles & vertical exaggeration.	11
<b>FIGURE 6:</b> Bare earth models generated with sun angle azimuths at 45° increments.	12
<b>FIGURE 7:</b> 1:3000 mapping grid, Nitra block.	14
<b>FIGURE 8:</b> Form line analysis example, Nitra project	15
<b>FIGURE 9:</b> Lineament analysis example, Nitra project.	16
<b>FIGURE 10:</b> Formline analysis results – Nitra project.	17
<b>FIGURE 11:</b> Total lineament data – Nitra Block.	18
<b>FIGURE 12:</b> Rose diagram of lineament azimuth data.	19
<b>FIGURE 13:</b> Lineament data coloured by predominant azimuth populations.	20
<b>FIGURE 14:</b> Lineament data coloured only NNW and ENE populations.	21
<b>FIGURE 15:</b> Lineament density interpolation raster, Nitra property.	22
<b>FIGURE 16:</b> Lineament length density interpolation raster, Nitra property.	22
<b>FIGURE 17:</b> Lineament intersection density interpolation raster, Nitra property.	23
<b>FIGURE 18:</b> Nitra soil geochemical survey location.	24
<b>FIGURE 19:</b> Robust hierarchical clustering results for Nitra block soil dataset.	25
<b>FIGURE 20:</b> Relationship between soil geochemical suites and NNW and ENE lineaments.	26
<b>FIGURE 21:</b> Interpretion of soil geochemical anomalies.	27
<b>FIGURE 22:</b> Eastern Nitra focused targets.	28
<b>FIGURE 23:</b> Block-scale target – Nitra project.	29
<b>FIGURE 24:</b> Eastern block-scale target and reduced to pole magnetic intensity data.	29

## **1.0 INTRODUCTION**

The following report summarizes the procedures to reprocess and analyze a Light Detection and Ranging (LiDAR) data set acquired over the Nitra project of Banyan Gold Corporation located in central Yukon, ~30 km northwest of the village of Mayo (**Fig. 1**). Banyan Gold Corp. is currently exploring these claims for intrusion-related gold mineralization which is typically strongly fault-controlled and occurs both within and exterior to causative intrusive bodies. The results of the analysis will assist future surface exploration and drilling campaigns.

The main objective of LiDAR image analysis work is to characterize and evaluate fault and lineament geometry that may control precious metal localization. To this end, a detailed lineament interpretation across the Nitra block using recently acquired LiDAR-generated digital elevation models is presented. The results of the analysis are used to:

- (a) Better understand structural controls on known zones of rock and soil geochemical anomalism, and,
- (b) Integrate with available geophysical and geochemical datasets to identify high priority target areas within the project area.

The report is divided into 5 parts, including:

- i) An outline of regional tectonic architecture that may be important for gold mineralization with the Nitra project area;
- ii) A summary of the LiDAR data and reprocessing procedures;
- iii) An outline of criteria used to carry out lineament analysis on the Nitra project LiDAR datasets;
- iv) A summary of the project-wide lineament analysis results;
- v) Target generation using available geophysics and soil geochemistry.

Data deliverables accompanying this report include newly reprocessed imagery data, a 0.35 m Digital Terrain Model (DTM) for the project area (GEOTIFF grid format); derivative bare earth hillshade products (ECW raster format) and vector file data in TAB format. All drafted maps and digital data products provided are generated using the NAD 83 CSRS datum and projected to UTM zone 8.

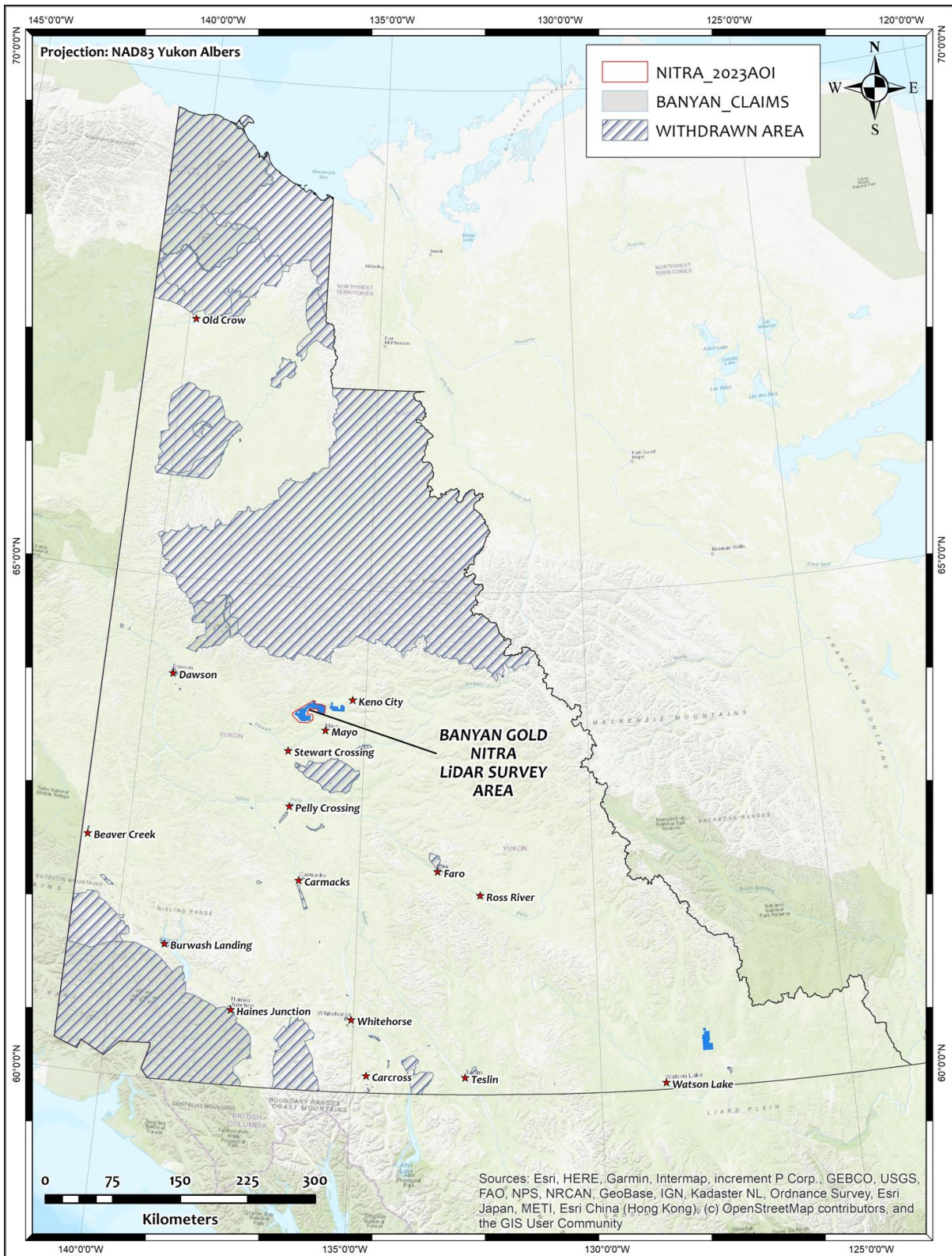


FIGURE 1: Location of Nitra project area, Banyan Gold Corp.

## **2.0 REGIONAL TECTONIC SETTING**

The Nitra project area is located in the north-central Selwyn basin, ~ 85 km east of the crustal-scale Tintina Fault (**Fig. 2**). The dominant stratigraphic units within the project area include clastic rocks of the Latest Proterozoic Hyland group and Mississippian Keno Hill Quartzite. Broadly NE-directed thrust deformation focused along the Robert Service Thrust has juxtaposed these two stratigraphic units within the project area.

Within the Selwyn Basin at least three major deformational events have occurred including from oldest to youngest:

1. **Jurassic-Cretaceous** north –northeast directed fold and thrust compressional deformation. This event is associated with formation of the Robert-Service thrust and intense transposition of bedding into mineral foliations. Deformation at this time was also associated with an early generation of quartz veining parallel to foliation development.
2. **Late Cretaceous** strike-slip and tensional deformation associated with the emplacement of the Tombstone intrusive suite. This event is a significant gold-mineralizing event throughout the Selwyn Basin and is likely associated with mineralization observed across the Banyan Aurmac property. Structures related to this strike-slip event re-activated pre-existing thrust faults, such as the Robert Service Thrust. Late Cretaceous structures over print early fold and thrust deformation.
3. **Earliest Cretaceous** deformation is associated with emplacement of the McQuesten intrusive suite. Additionally, gold mineralizing occurring during this deformation event resulted in formation of the Tiger, Osiris and Conrad deposits and the Venus occurrence. Deformation related to these events is thought to be transpressional and involves SW-directed fold and thrusting as well as strike-slip faulting.

Emplacement of intrusions related to the Tombstone Intrusive suite was likely facilitated by dextral strike-slip displacement along the Tintina Fault during the Early Cretaceous. **Figure 3** illustrates a highly simplified but plausible regional tectonic framework that can be used to better understand gold occurrences occurring between Mayo and Keno City.

Within this framework, two crustal-scale bounding faults facilitate overall dextral displacement across the Selwyn Basin during the Early Cretaceous. Gold mineralization associated with Tombstone intrusives are focused along the internal structures that accommodate displacement along these major bounding fault zones. These accommodating structures also permit emplacement of intrusive bodies. Note the broad NW-SE

long axes of the mapped occurrences of Early Cretaceous Intrusives. These areas represent zones of crustal extension.

The Nitra property is situated between larger regional linear features that converge and likely intersect where the Aurmac, Airstrip and Powerline deposits occur. The location of the Robert-Service thrust plays an important role in controlling gold mineralization in these zones and should also be considered important for the Nitra block. The Robert-Service thrust continuous into the NE portion of the Nitra claims and it is unclear where this structure continues westward. This structural and subordinate higher thrust stack level faults may be reactivated during the emplacement of the Tombstone Intrusive suite and be important sites of gold localization. Importantly, several Cretaceous Intrusions are known to outcrop within the Nitra block.

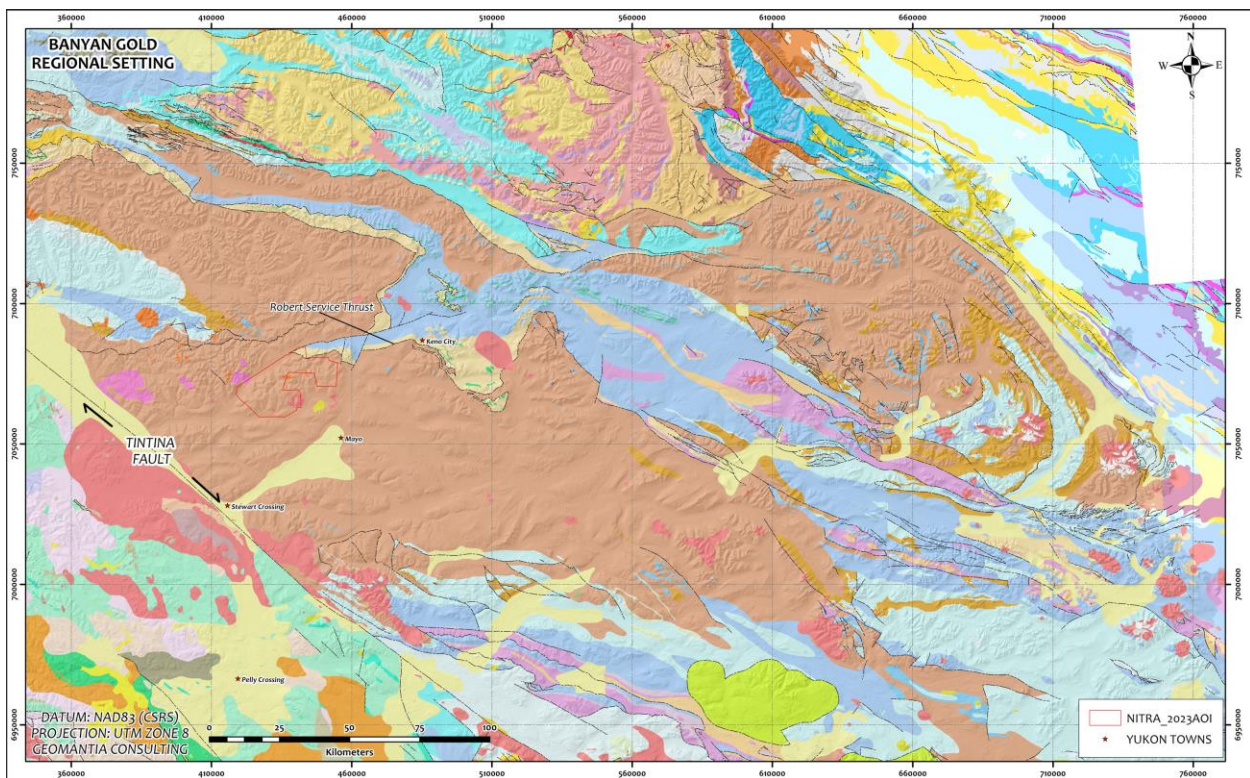


**FIGURE 2:** Regional geological setting of the Nitra Property, Banyan Gold Corp.

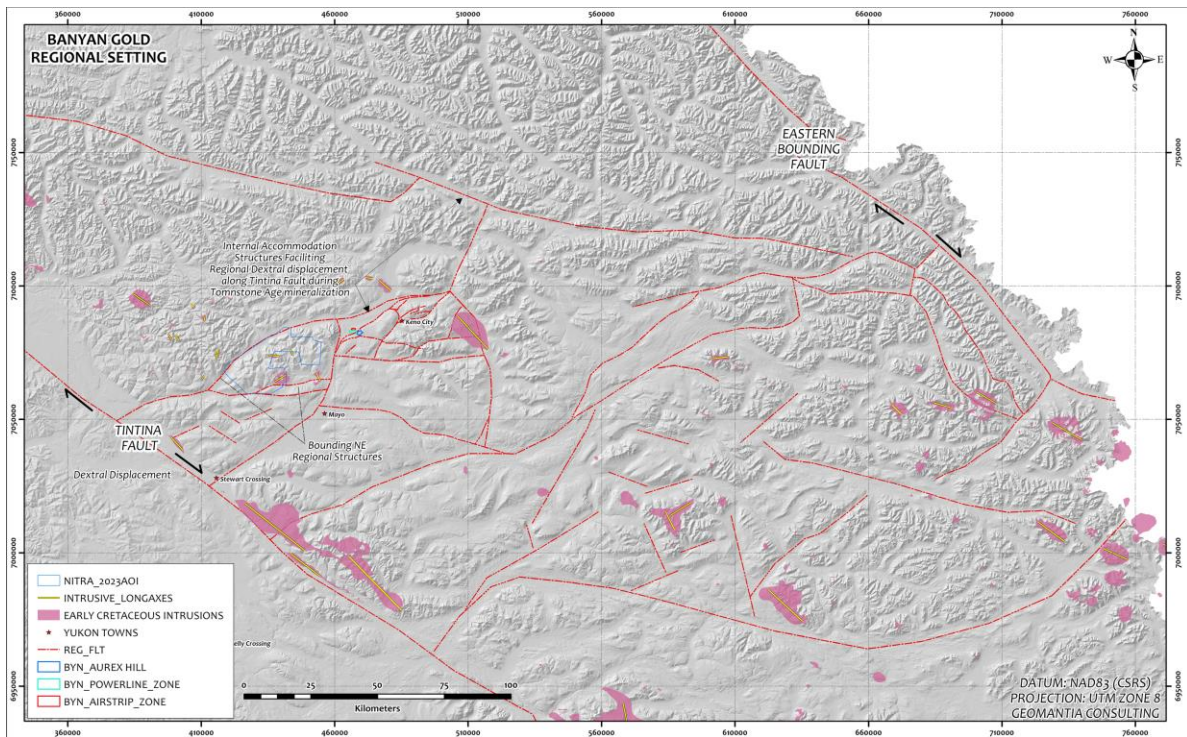


**FIGURE 3:** Simplified Early Cretaceous tectonic setting of the Nitra property, Banyan Gold Corp.

### 3.0 LIDAR REPROCESSING

An airborne LiDAR survey was carried out in summer 2022 over the Nitra project by McElhanney Ltd. Deliverables were provided to Banyan Gold Corp. in NAD83 (CSRS) horizontal datum and projected to UTM zone 8. The Canadian vertical datum CGVD 2013 was used to determine elevation in orthometric height.

The raw LiDAR data (487 las files) were acquired from McElhanney Ltd. for the Nitra property and reprocessed to generate a 0.35 m resolution Digital Terrain Model (DTM). The equation below was used to determine ideal DTM resolution.

**Lidar density and DEM resolution**

- average of 1 Lidar pulse per DEM pixel
- Point density (e.g., 8 pulses per square meter)
- Point spacing (e.g., 50 cm)

$$PS = \text{SQRT}(1/PD)$$

Example: 8 pulses / meter<sup>2</sup> = 0.35 meters

The higher resolution DTM dataset permitted improved clarity of surface features and significantly aided in subsequent lineament interpretations (**Fig. 4**).

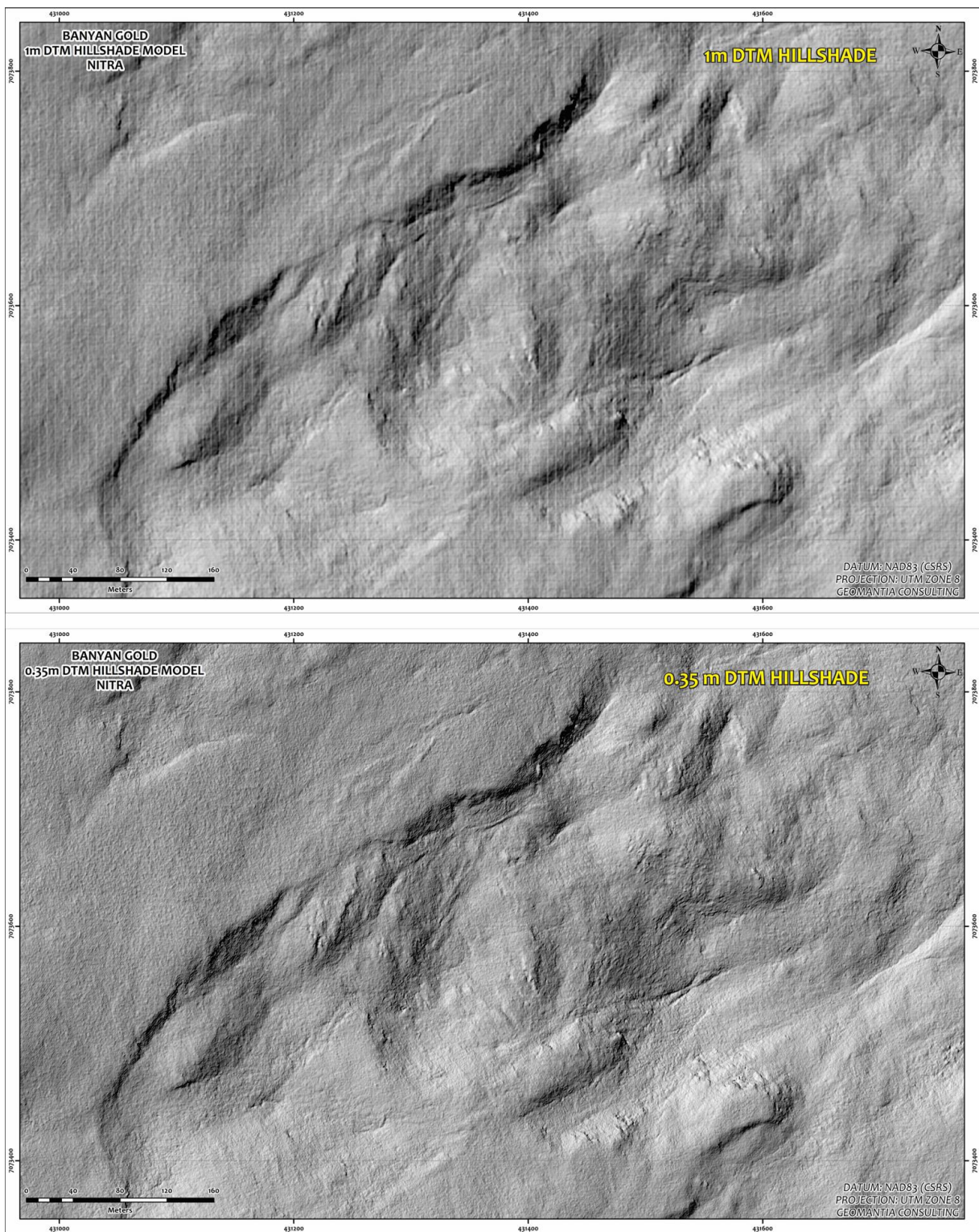


**FIGURE 4:** Comparison of 1 m vs 0.35 m resolution DTMs for Nitra project.

This 0.35 m DTM was then used to generate three suites of hillshade models with different sun illumination angles ( $10^\circ + VE = 3$ ;  $45^\circ + VE = 1$  &  $45^\circ + VE = 3$ ; **Fig. 5**). Additionally, for each of the two sun illumination angles, 8 different hillshade models were generated at  $45^\circ$  sun azimuth increments ( $0^\circ$ ,  $45^\circ$ ,  $90^\circ$ ,  $135^\circ$ ,  $180^\circ$ ,  $225^\circ$ ,  $270^\circ$  and  $315^\circ$ ; **Fig. 6**). Variations in both sun angles (from the horizon) and sun azimuths illuminate different topographic features that are present in the DTM but are not visible to the human eye. Working with each different hillshade dataset provides a comprehensive method in which to carry out lineament interpretations.

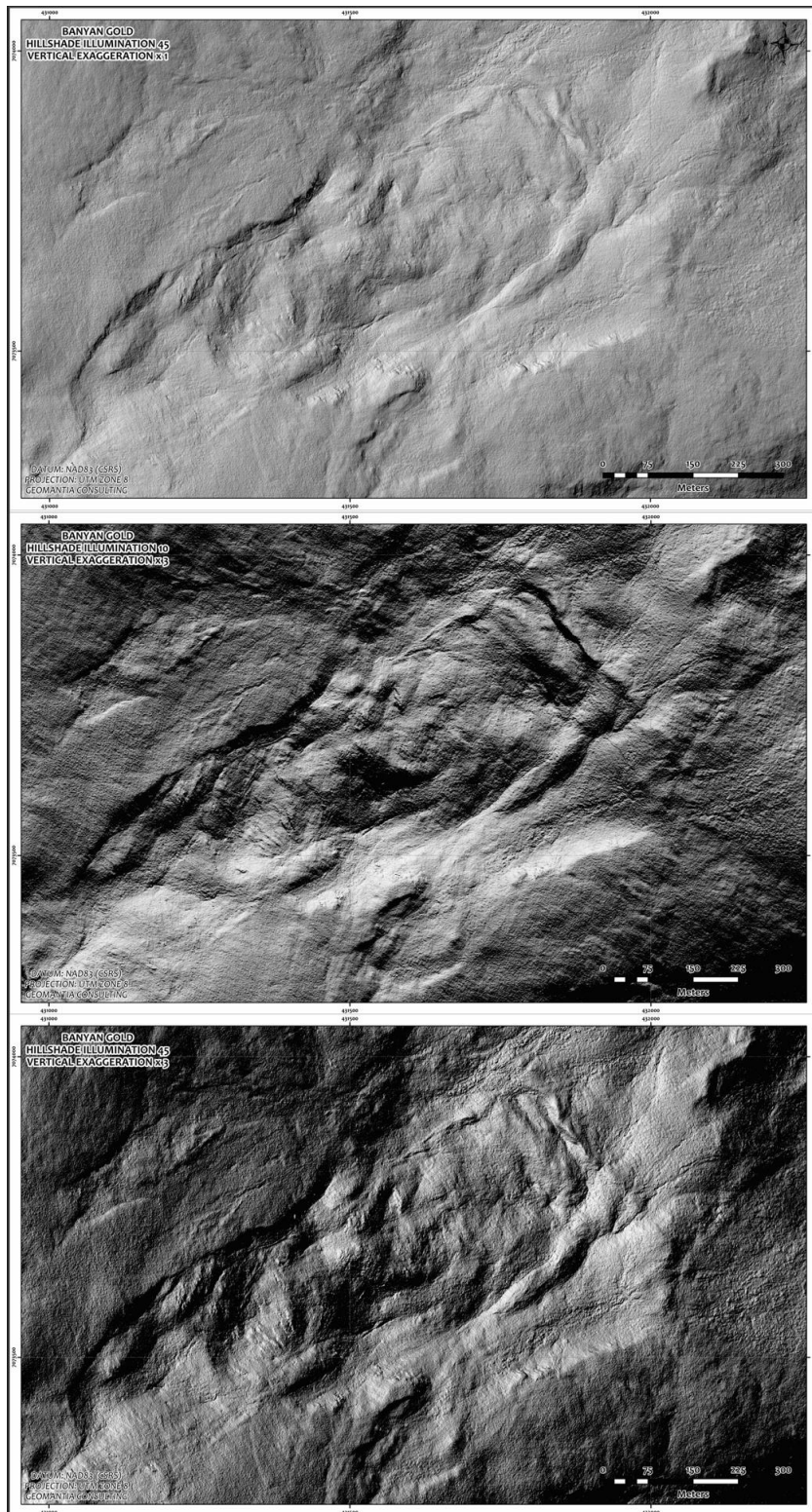


**FIGURE 5:** Three bare earth hillshade models with 2 different sun illumination angles and vertical exaggeration levels.

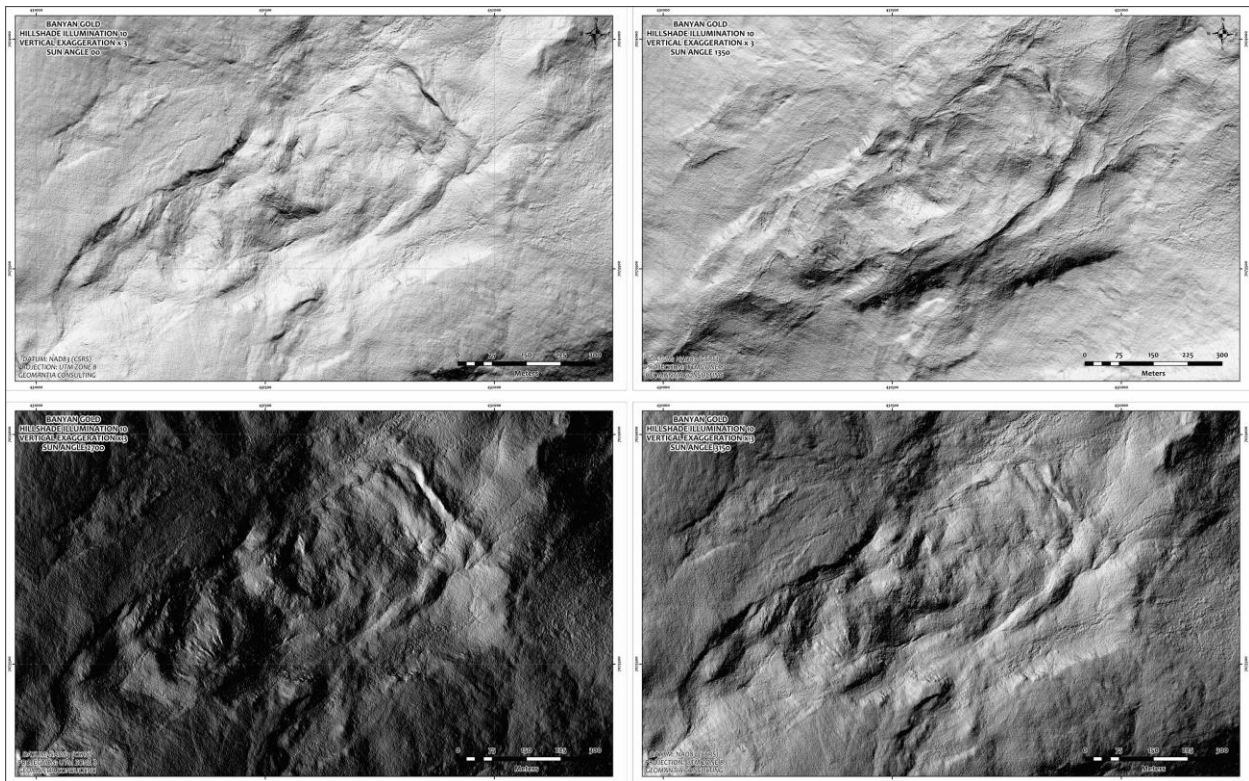


FIGURE 6: Bare earth models generated with sun angle azimuths at 45° increments.

#### 4.0 LiDAR ANALYSIS PROCEDURES

Subsequent to reprocessing of the LiDAR point cloud, the new imagery products were used to conduct a lineament interpretation across the Nitra project (~444 km<sup>2</sup>). The following procedures were adopted:

- ▲ Generation of 1: 3000 grid that encompasses the mapping area (Fig. 7).
- ▲ Systematic mapping of (a) bedding form lines and (b) all interpreted faults and lineaments.
- ▲ Lineament density and length interpolation analysis.
- ▲ Lineament azimuth analysis and rose diagram reviews.
- ▲ Identification of the anomalously dense structural networks.
- ▲ Comparison to soil geochemical and geophysical datasets and target generation.

Form lines represent bedding trace lines which highlight the general strike of sedimentary rocks in a given area. **Figure 8** is an example of a form line interpretation in sedimentary rocks in the Nitra project area. Systematic form line interpretations help to identify areas of folding and zones of structural discontinuity.

Lineaments are considered to be any straight line topographic feature that can be clearly identified in hillshade imagery which may represent faults, fractures and joints. **Figure 9** shows an example of lineaments visible in the Aurmac project hillshade imagery.

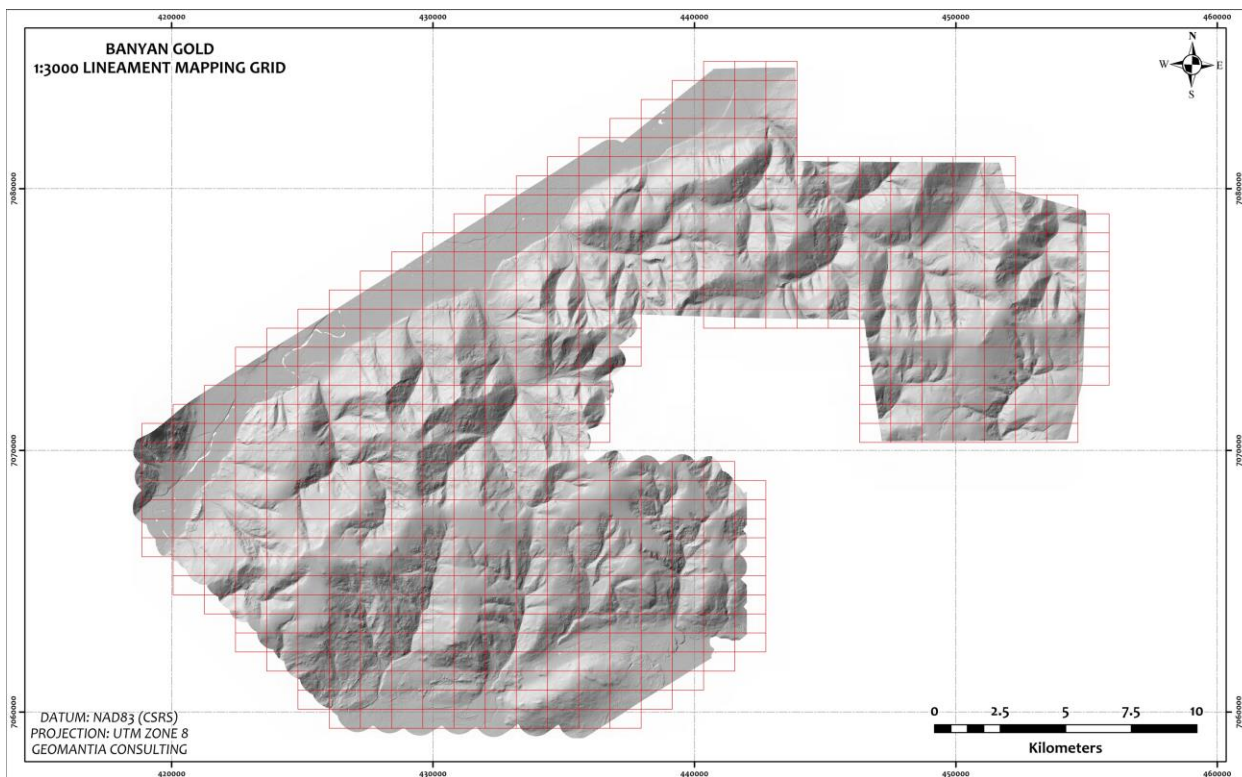


FIGURE 7: 1:3000 mapping grid, Nitra block.

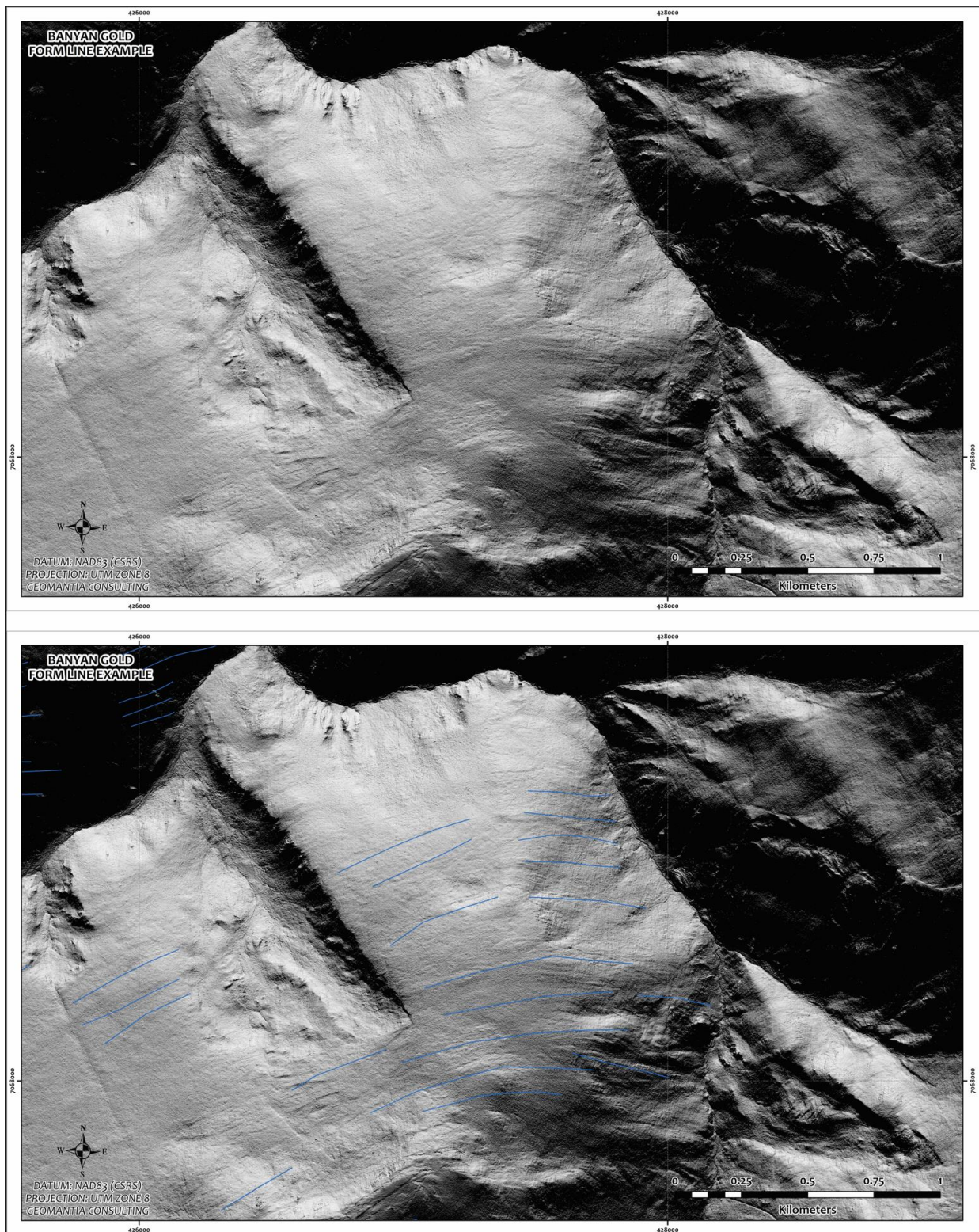


FIGURE 8: Form line analysis example, Nitra project

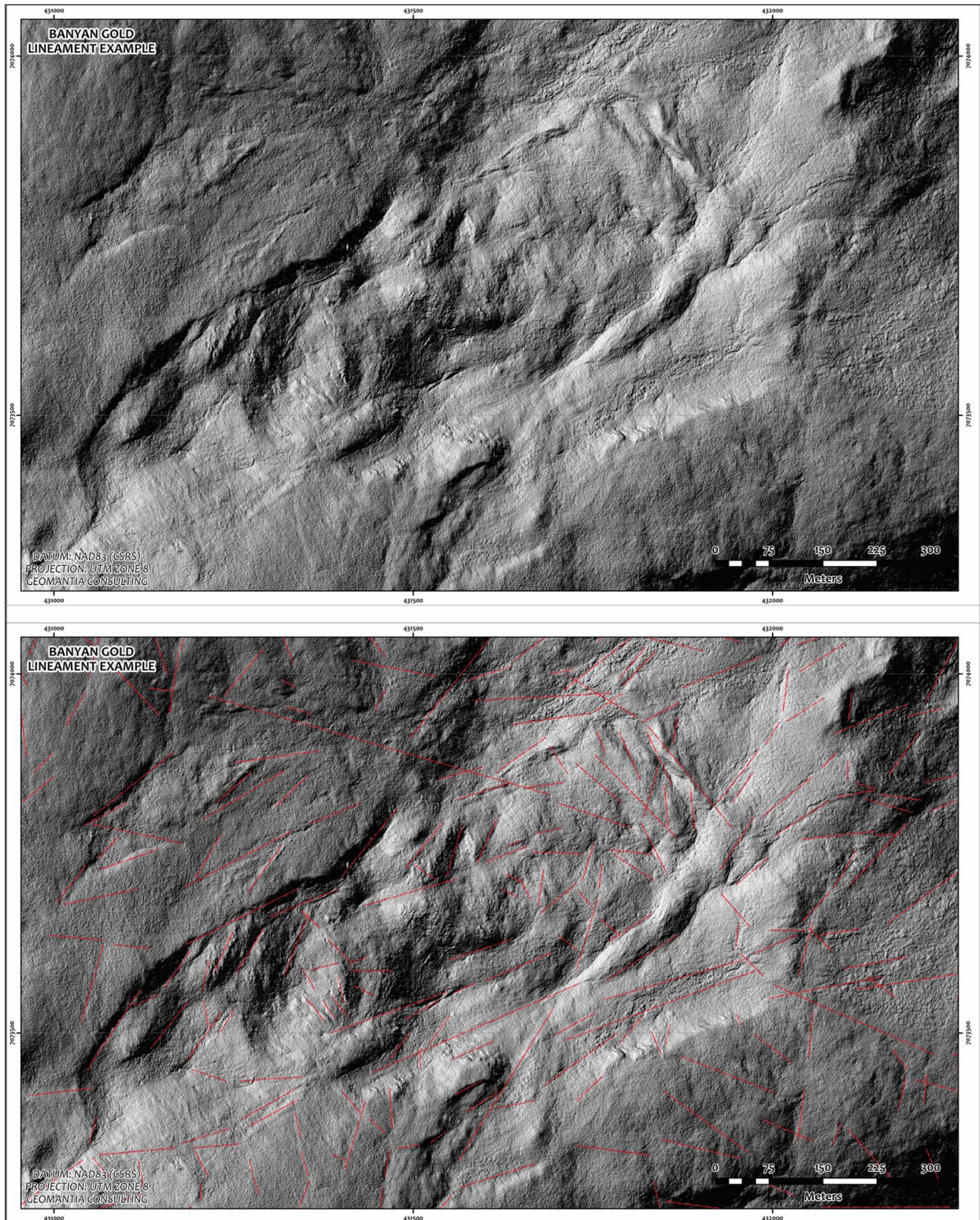
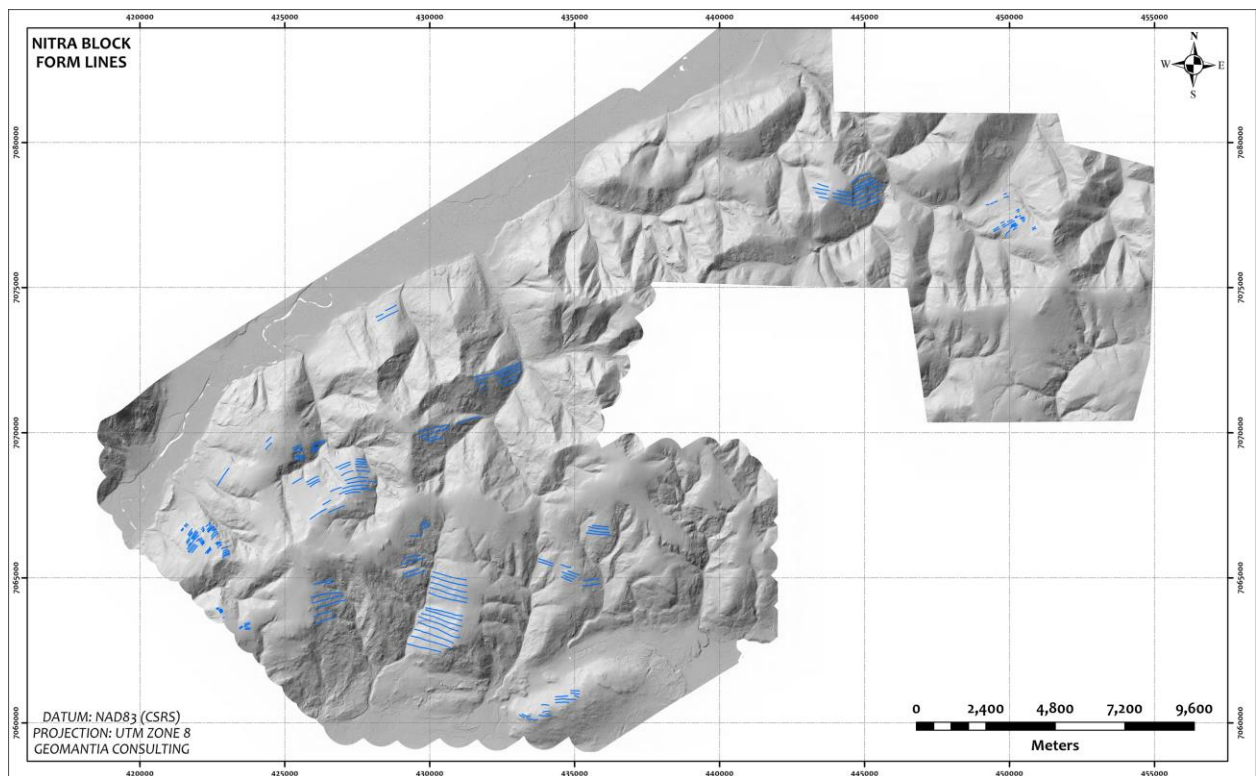


FIGURE 9: Lineament analysis example, Nitra project.

## 5.0 LiDAR MAPPING RESULTS – NITRA PROJECT AREA

### FORMLINE MAPPING RESULTS

Sedimentary rocks within the Nitra project strike broadly E-W and NE-SW (**Fig. 10**). The widespread extensive till and regolith cover made form line analysis across the Nitra block difficult. 1: 5000 scale block scale geological mapping may be useful to identify (i) the continuation of the Robert-Service Thrust; (ii) higher thrust stack level faults that may have been reactivated and (iii) folding in the Hyland Group stratigraphic package.

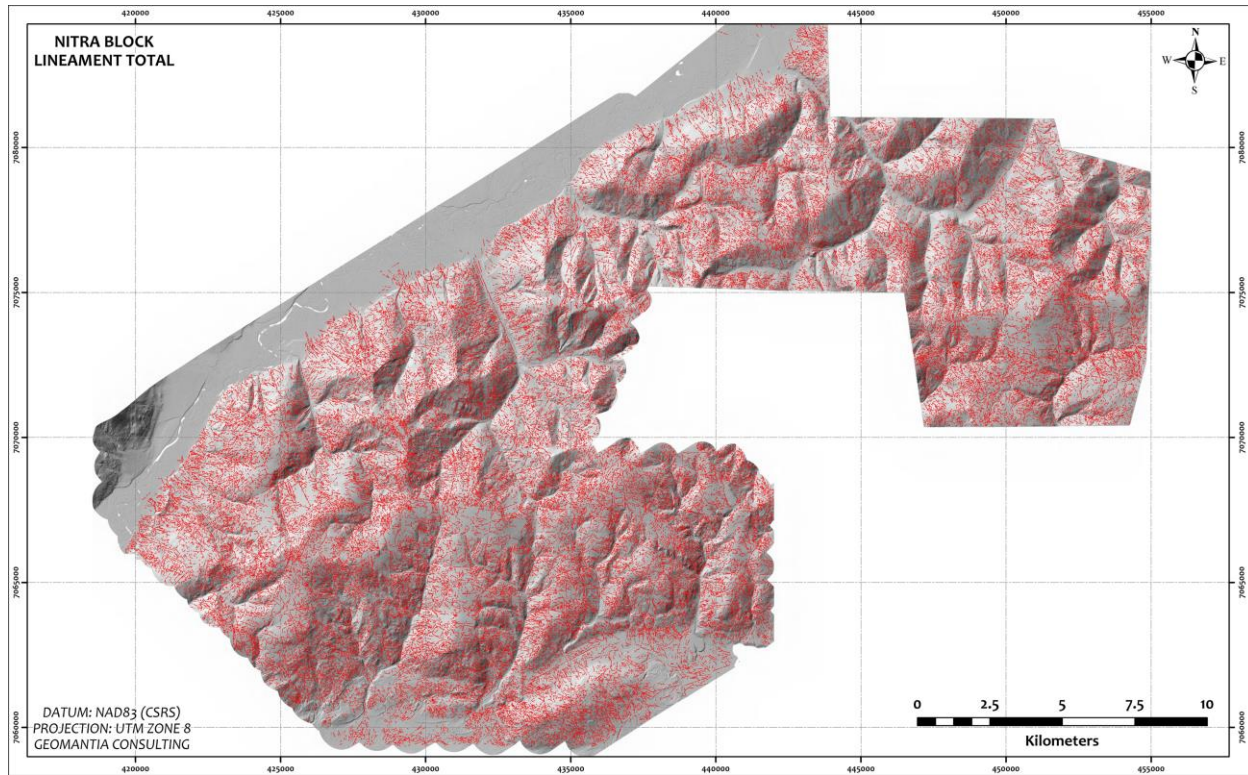


**FIGURE 10:** Formline analysis results – Nitra project.

### LINEAMENT MAPPING RESULTS

Systematic mapping of lineaments within each 1:3000 scale grid square resulted in generation of 78468 individual linear features within the Nitra block (**Fig. 11**). Lineament azimuth data were analyzed using a rose diagram (**Fig. 12**). The diagram demonstrates the presence of two dominant populations including NNW (average  $340^{\circ}$ ) and WNW (average  $290^{\circ}$ ), and one subordinate population at average azimuth of  $075^{\circ}$ . These average lineament orientations are consistent with the lineament populations observed within the Aurmac

project area. An important distinction is the much greater concentration of ENE trending lineaments, which is known to be an important orientation for the mineralization at Powerline.



FIGURE

FIGURE 11: Total lineament data – Nitra Block.

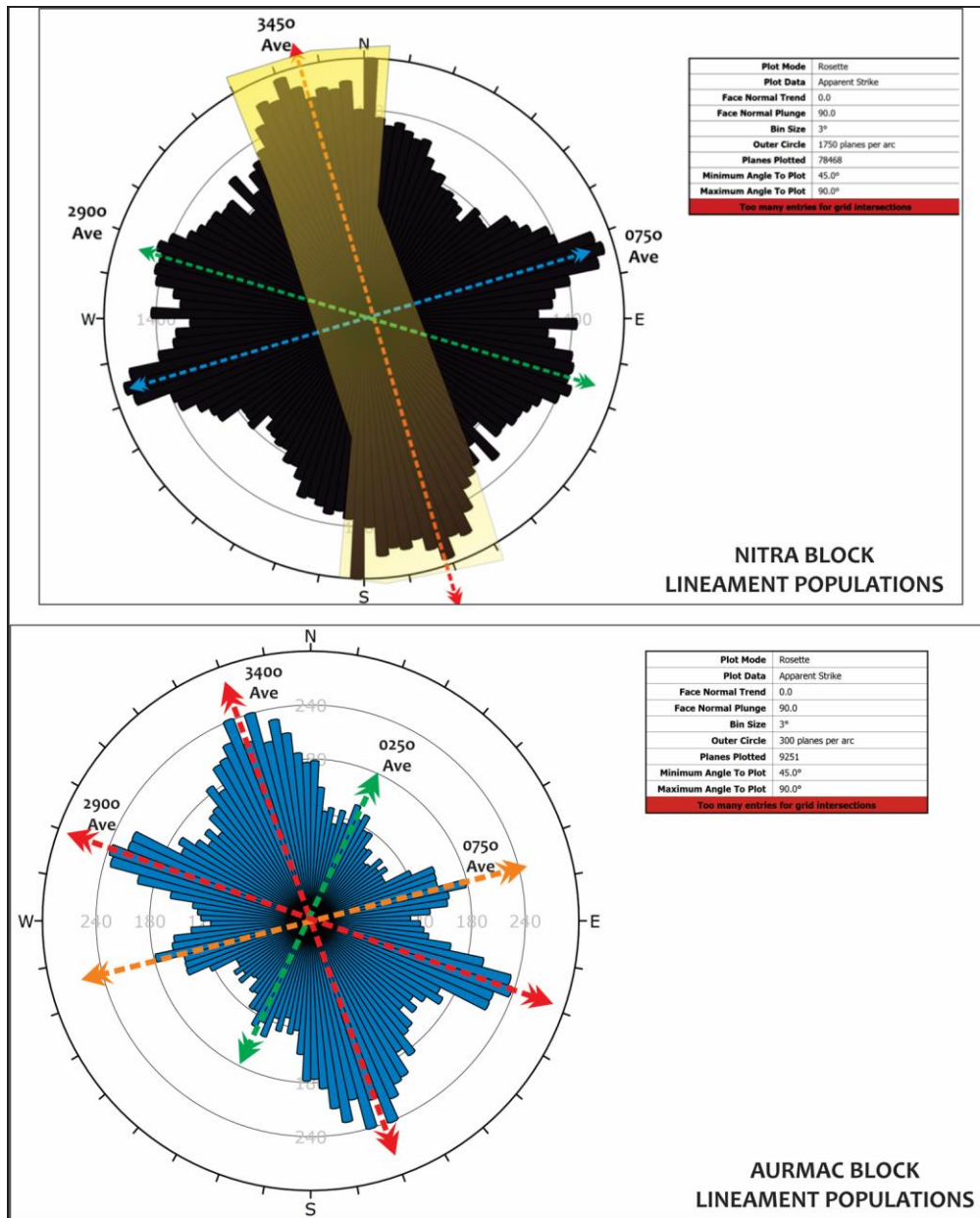
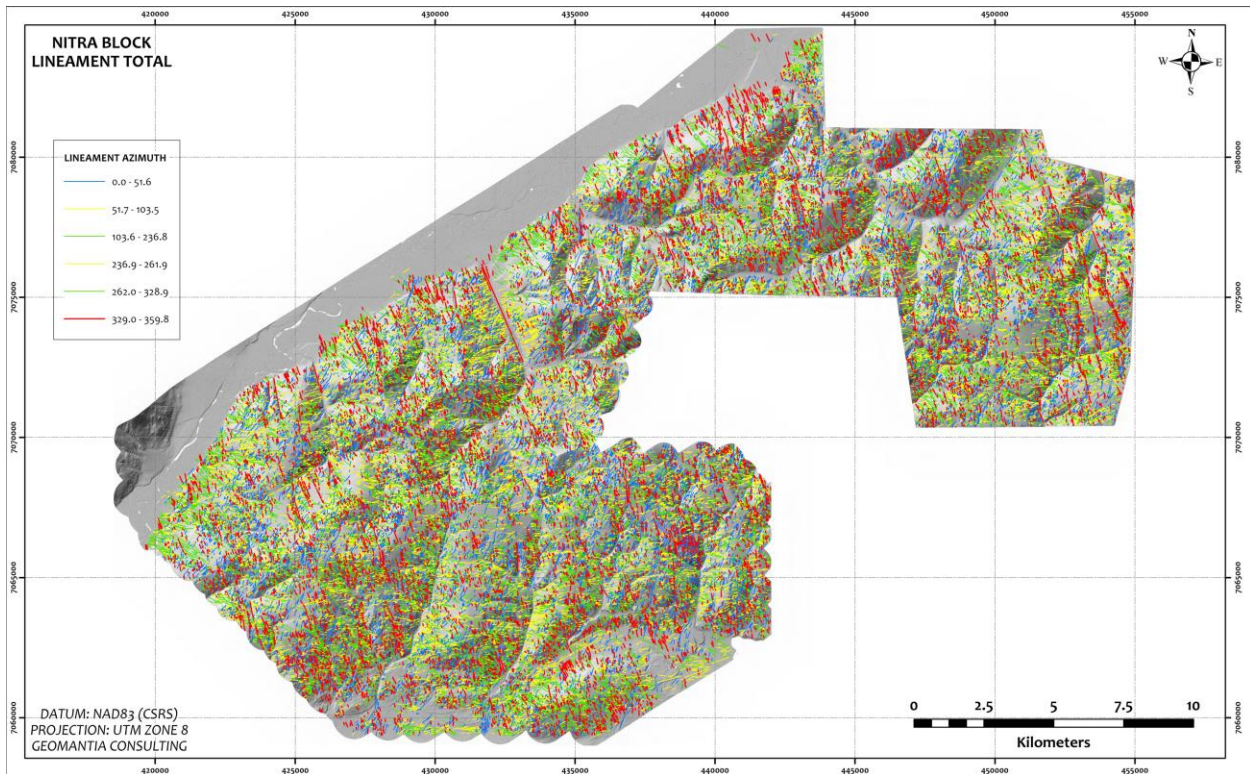


FIGURE 12: Rose diagram of lineament azimuth data, Nitra block compared to Aurmac Block.

**Figure 13** illustrates the distribution of lineaments coloured by main directional domains (NNW, NE, ENE and NW). Colorization by azimuth populations as revealed by rose diagram analysis assists to visualize and identify regions/areas dominated by a prevailing structural fabric. For the Nitra block, **Figure 12** suggests a prevalence of NNW trending and through-going structures on the NE half of the claim block and ENE trending lineaments in the south-western portion of the project area.



**FIGURE 13:** Lineament data coloured by predominant azimuth populations – Nitra Block.

When only ENE and NNW populations are examined (*ENE known regional mineralizing orientation and NW-NNW long axes of late Cretaceous intrusions*), this trend becomes more evident (**Fig. 14**). Intersection points between these structures maybe higher potential exploration targets.

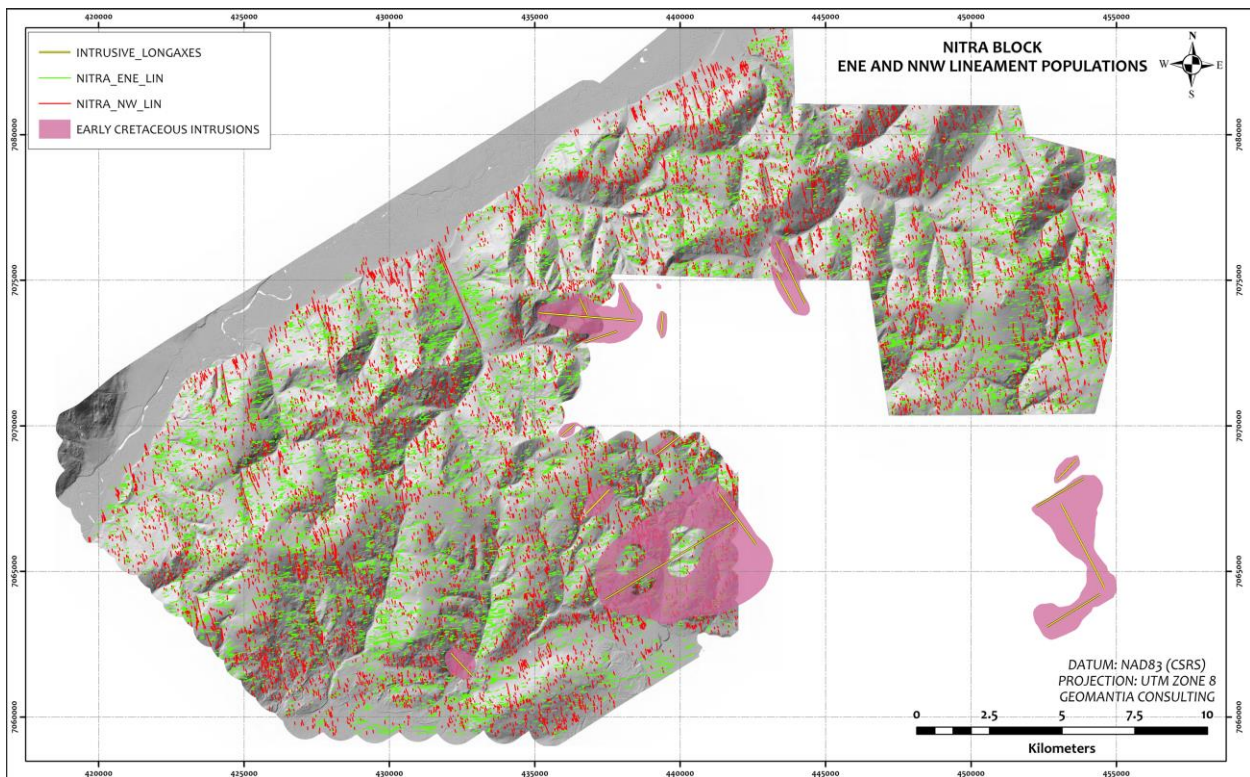


**FIGURE 14:** Lineament data coloured only NNW and ENE populations – Nitra Block.

A lineament density kernel interpolation grid is a useful way to visualize areas with high fault density that may represent favorable areas to localize gold mineralization (i.e. an appropriate plumbing system). Areas classified with warm colours (yellow to red) represent dense networks of different lineament populations. Lineament length interpolation rasters illustrate where continuous through-going structures are well-developed. Areas classified with warm colours (yellow to red) represent zones with a high likelihood of the presence of through-going fault system. Lineament density and lineament length interpolation rasters are presented in **Figures 15 and 16**. A final lineament intersection interpolation raster is presented in **Figure 17** and identifies important target areas where NNW and ENE structures intersect (lineament intersection density).

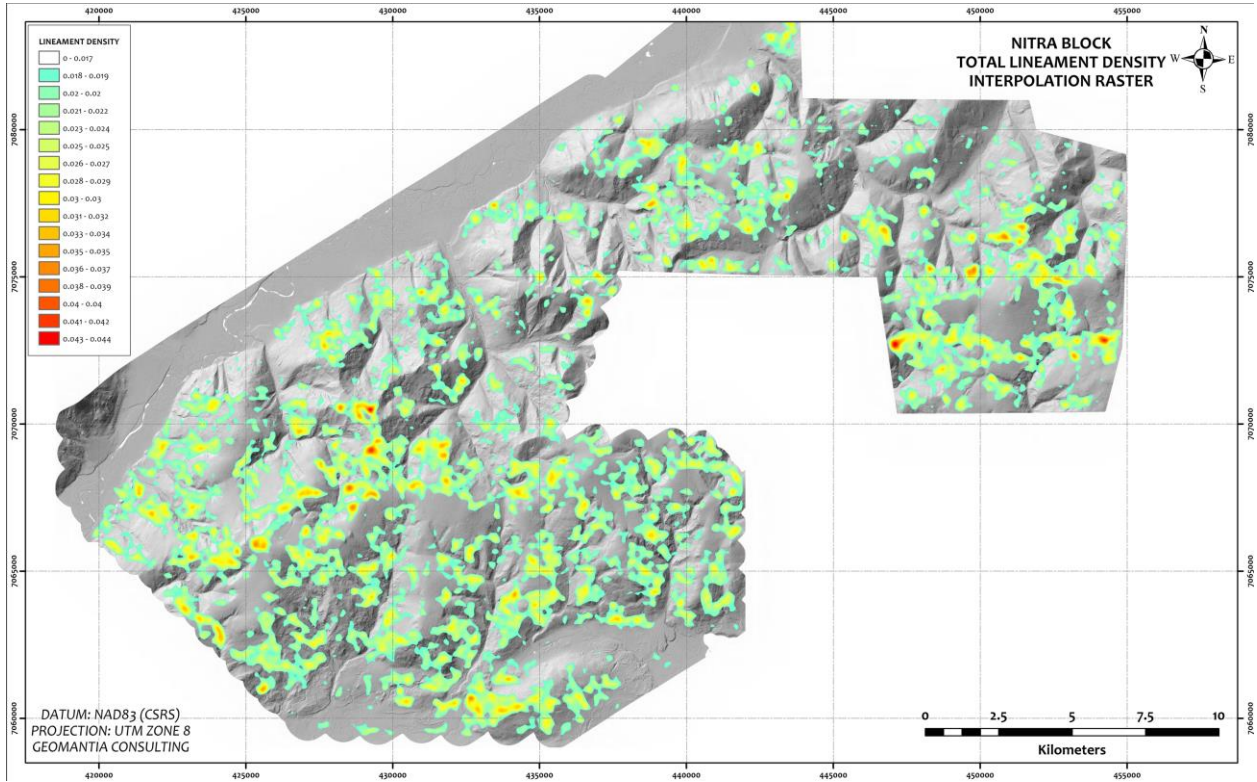


FIGURE 15: Lineament density interpolation raster, Nitra property.

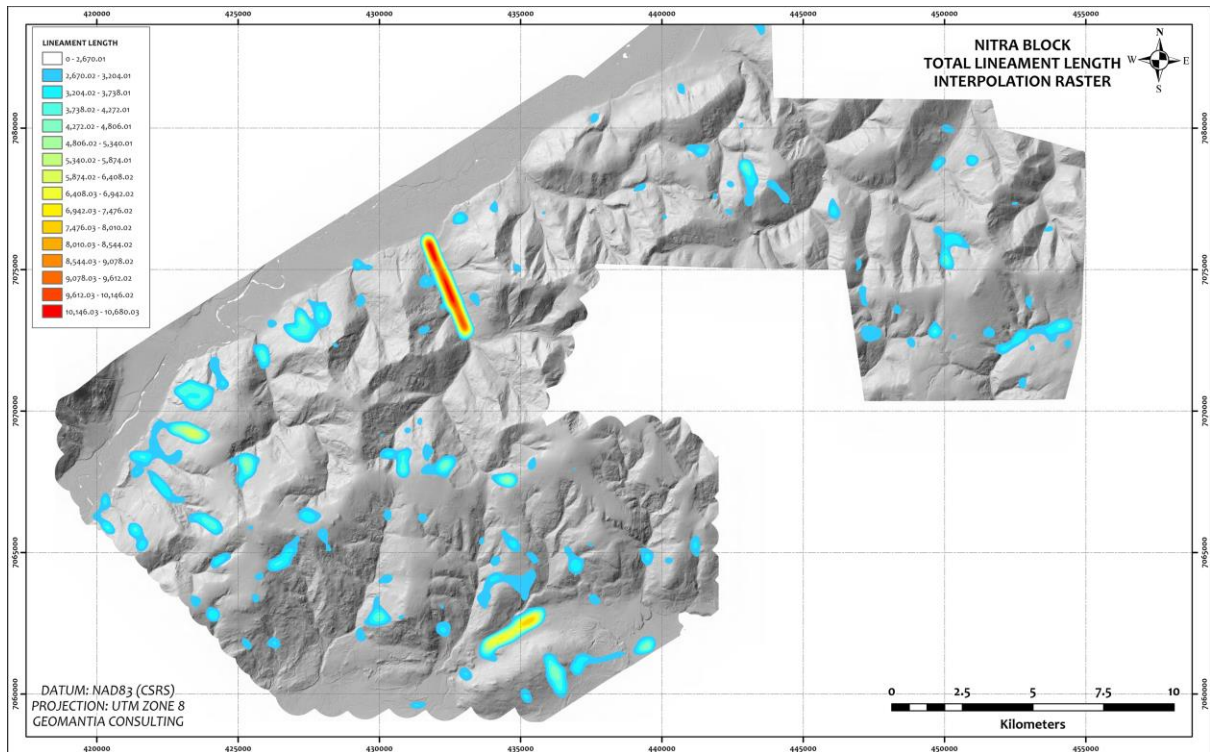
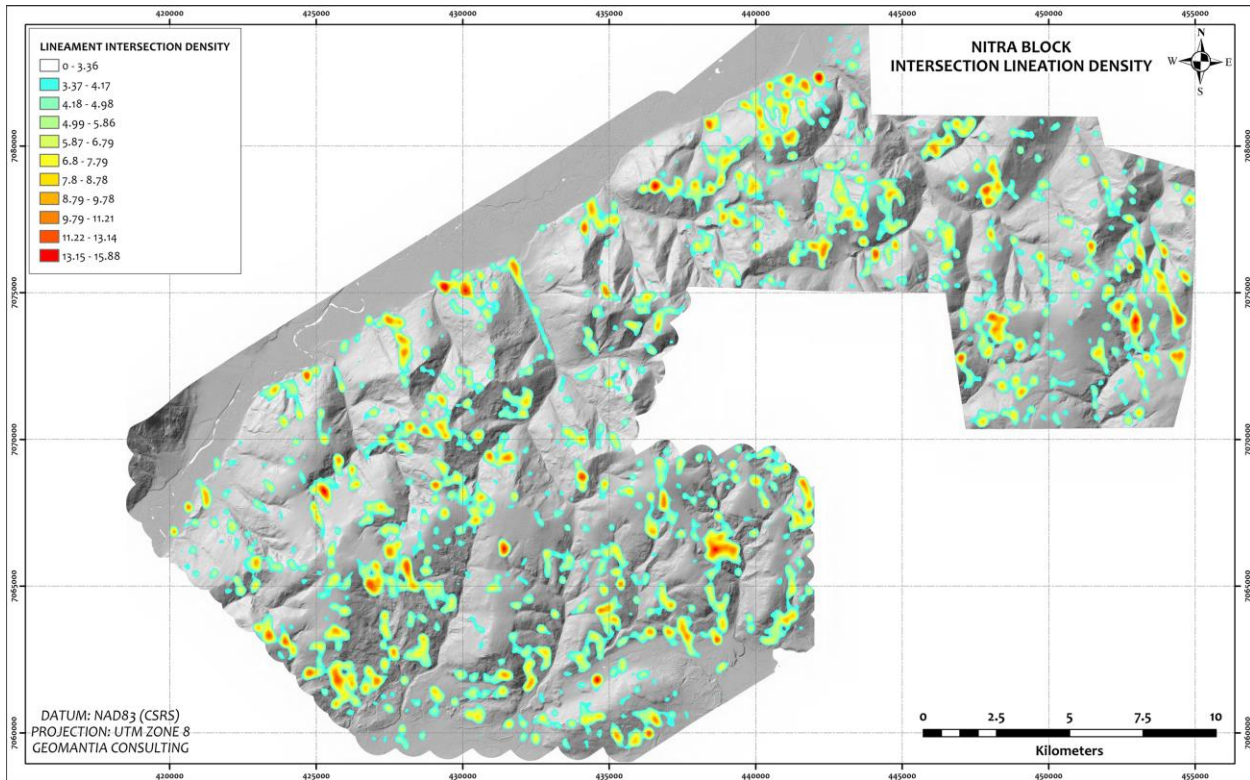


FIGURE 16: Lineament length density interpolation raster, Nitra property.



**FIGURE 17:** Lineament intersection density interpolation raster, Nitra property.

Lineament analysis for the Nitra block reveals that a strong prevailing NNW-NW trending fabric characterizes the NE half of the project area. This NNW dominant trend also parallels the long axes of several mapped Late Cretaceous Intrusions in the area. A secondary prevailing ENE-trending fabric is also present within the NE Nitra block. This orientation is not only a favourable regional mineralizing orientation but is also parallel to axes of neighbouring Late Cretaceous intrusions. The similarity in orientations suggests a relationship between these two main lineament populations (NNW and ENE) and fault geometry that permitted emplacement of Late Cretaceous intrusions. Intersection points as well as through-going NNW and ENE trending lineaments should be high priority prospecting and mapping targets.

The SW half of the Nitra block is characterized by less through-going NNW lineaments and more concentrations of ENE lineaments. The prospectivity of this geometric setting is unclear without further geochemical data and follow-up prospecting.

## 6.0 TARGETING

A soil geochemical data set (n=18523) was made available to review and integrate with the lineament analysis for the Nitra block (**Fig. 18**).

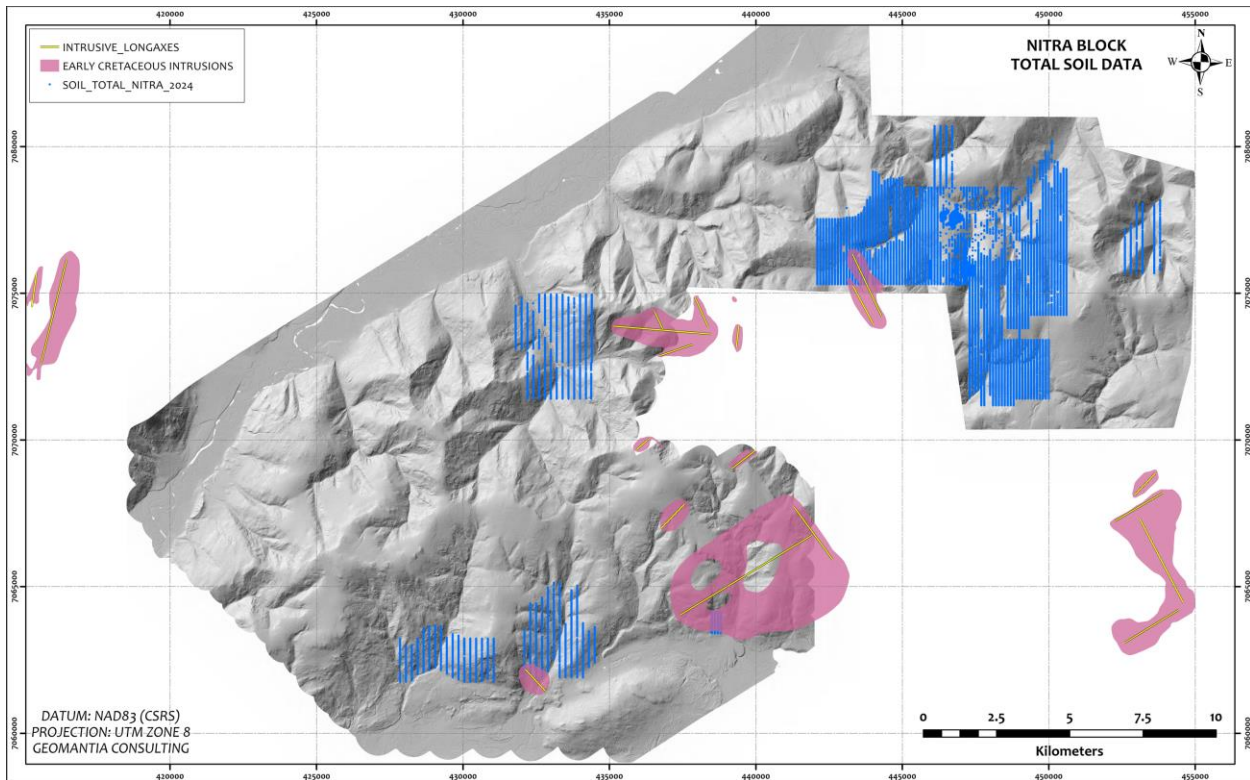


**FIGURE 18:** Nitra soil geochemical survey location.

A Spearman rank correlation matrix is presented in **Table 1** and indicates two main groups of correlations are present, including:

1. **Au-Ag-As-Sb**
2. **Cu-Pb-Zn+/-Ag-Ni-Co**

A robust hierarchical cluster analysis conducted on the data also indicates three distinct geochemical groupings are present in the soil data set for the dominant metal and pathfinder elements selected (**Fig. 19**). The main groupings are broadly consistent with the spearman correlation matrix with the exception of a Mo-Bi association with Pb.

Spearman - 18523 rows - Pair	Au_PPM	Ag_PPM	As_PPM	Sb_PPM	Bi_PPM	Mo_PPM	Cu_PPM	Pb_PPM	Zn_PPM	Ni_PPM	Co_PPM	W_PPM	Hg_PPM
Au_PPM	1	0.46	0.67	0.5	0.53	-0.012	0.42	0.44	0.41	0.35	0.34	0.16	0.2
Ag_PPM	0.46	1	0.6	0.35	0.5	0.087	0.38	0.59	0.54	0.39	0.37	0.076	0.14
As_PPM	0.67	0.6	1	0.57	0.66	0.11	0.4	0.62	0.53	0.41	0.39	0.17	0.027
Sb_PPM	0.5	0.35	0.57	1	0.42	0.036	0.46	0.5	0.44	0.44	0.42	0.14	0.084
Bi_PPM	0.53	0.5	0.66	0.42	1	0.13	0.46	0.61	0.49	0.4	0.41	0.076	0.11
Mo_PPM	-0.012	0.087	0.11	0.036	0.13	1	0.019	0.087	0.12	0.013	0.026	0.17	0.05
Cu_PPM	0.42	0.38	0.4	0.46	0.46	0.019	1	0.57	0.75	0.88	0.82	-0.099	0.14
Pb_PPM	0.44	0.59	0.62	0.5	0.61	0.087	0.57	1	0.7	0.56	0.58	-0.06	0.1
Zn_PPM	0.41	0.54	0.53	0.44	0.49	0.12	0.75	0.7	1	0.8	0.8	0.0053	0.07
Ni_PPM	0.35	0.39	0.41	0.44	0.4	0.013	0.88	0.56	0.8	1	0.9	-0.13	0.054
Co_PPM	0.34	0.37	0.39	0.42	0.41	0.026	0.82	0.58	0.8	0.9	1	-0.1	0.066
W_PPM	0.16	0.076	0.17	0.14	0.076	0.17	-0.099	-0.06	0.0053	-0.13	-0.1	1	0.084
Hg_PPM	0.2	0.14	0.027	0.084	0.11	0.05	0.14	0.1	0.07	0.054	0.066	0.084	1

TABLE 1: Spearman rank correlation matrix for Nitra project soil data.

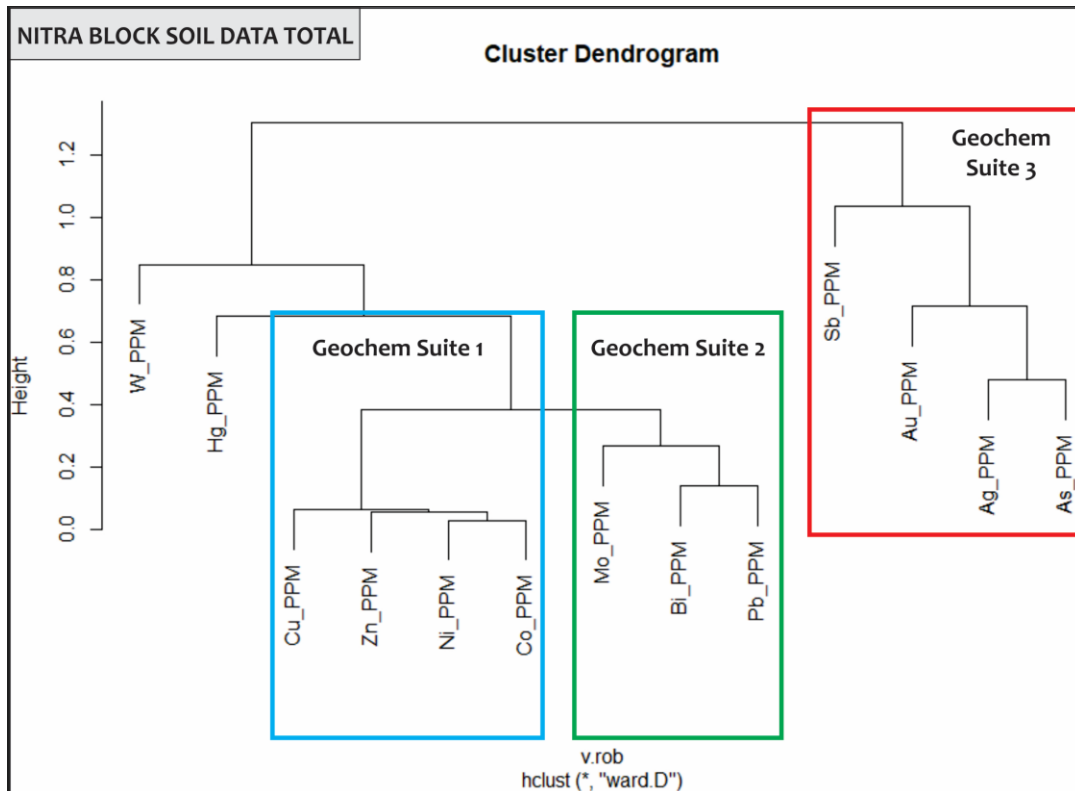
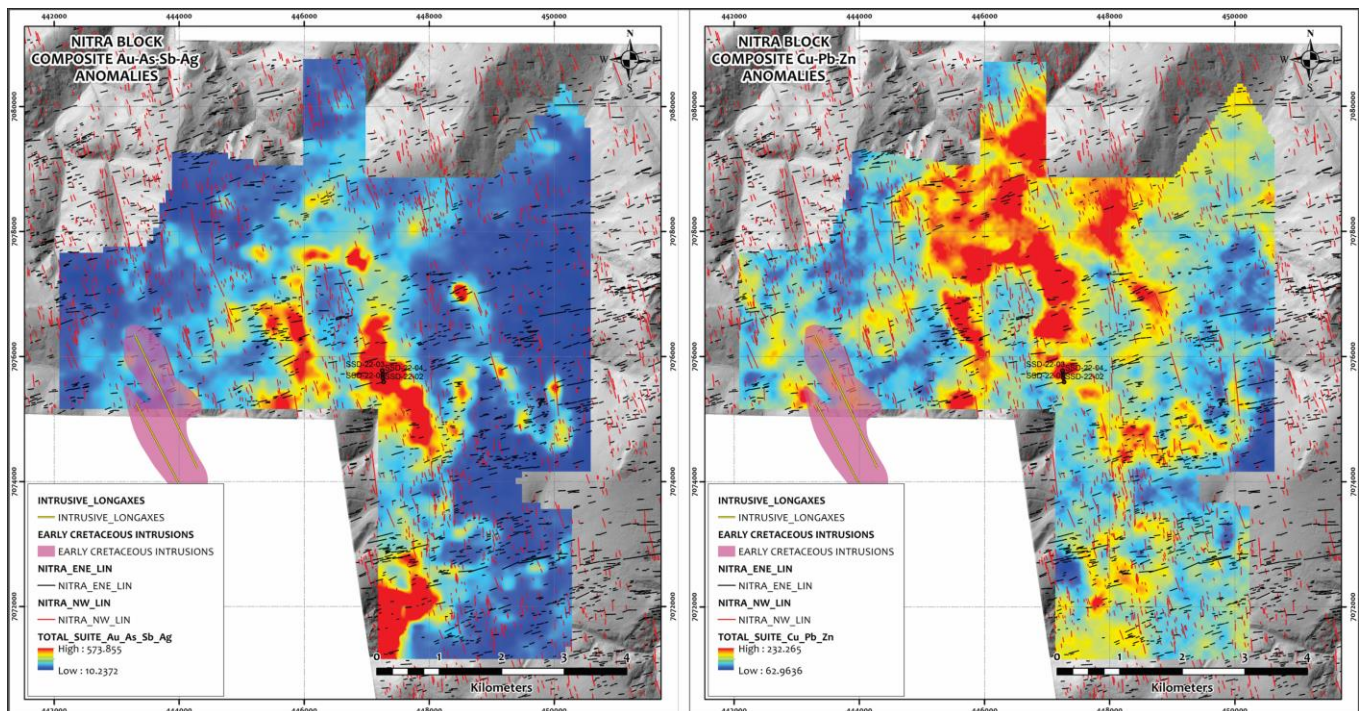


FIGURE 19: Robust hierarchical clustering results for Nitra block soil dataset.

A review of the soil geochemical data in geographical space reveals (i) differences between areas of anomalous metal concentrations and (ii) an important relationship to lineament orientations. **Figure 20** illustrates two composite geochemical anomaly interpolation plots for (a) **Au-Ag-As-Sb** and (b) **Cu-Pb-Zn**. Each hotspot area represents areas with coincident anomalies for each suite of interest.



**FIGURE 20:** Relationship between soil geochemical suites and NNW and ENE trending lineaments.

Important observations from the integration of soil geochemistry and lineament analysis include:

1. The two **geochemical suites** are large **geographically distinct** from each other with Cu-Pb-Zn anomalism occurring in the north of the soil grid area and Au-As-Ag-Sb anomalism more central and south in the grid area.
2. The interpolated shape of the soil anomalies for both geochemical suites is predominantly NNW consistent with the long axis orientation of the adjacent Late Cretaceous Intrusion.
3. A secondary ENE shorter orientation is also present in the soil geochemical interpolation plots suggesting a very close relationship between faulting and the shape of the soil anomalism.

**Figure 21** suggests a relationship between the soil geochemical suites in terms of zonation outward from a potential causative intrusion to the west of the soil grid.

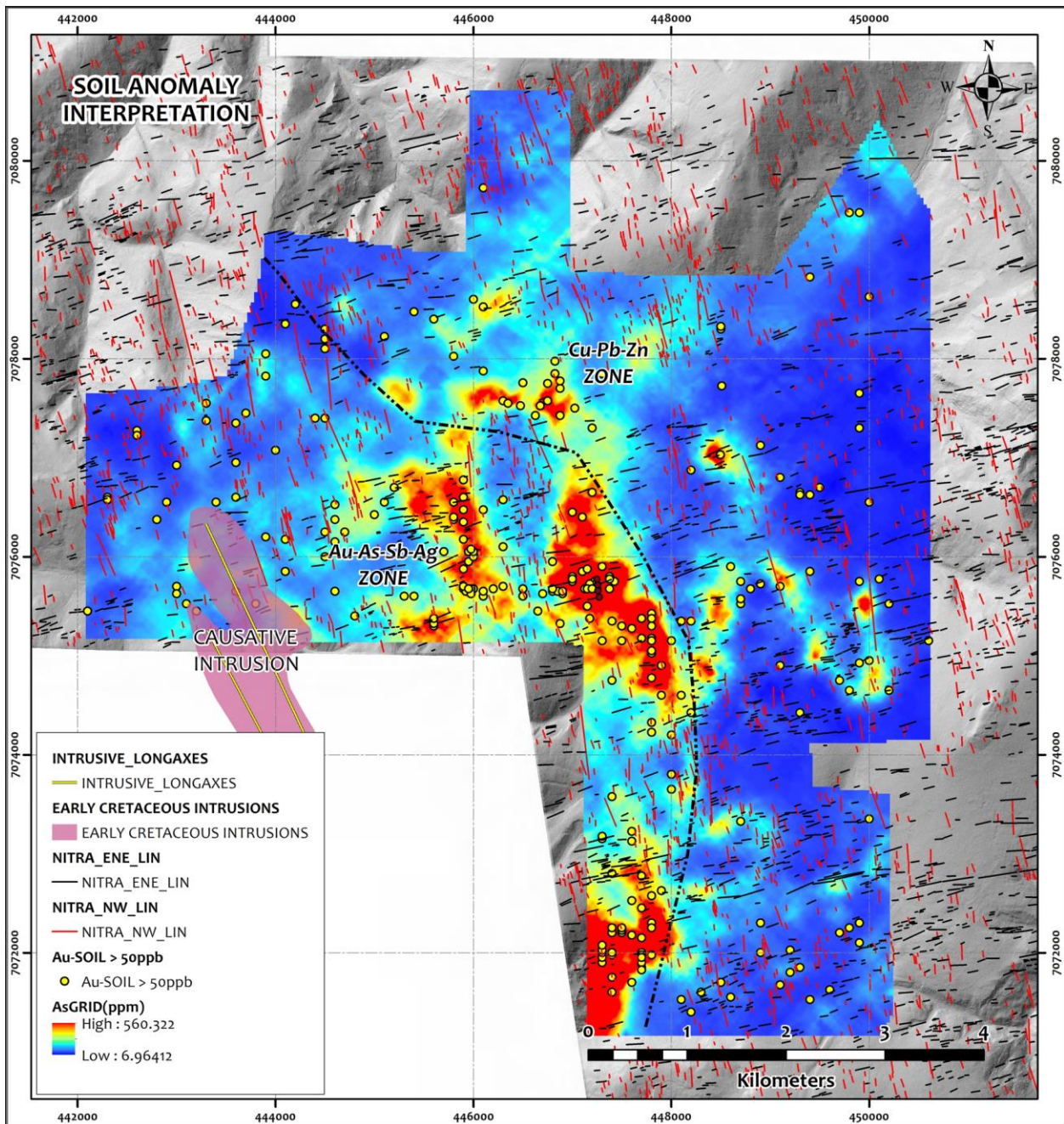


**FIGURE 21:** Interpretation of soil geochemical anomalies as a result of zonation related to distance from Late Cretaceous intrusion.

Integration of lineament and soil geochemical data for the Nitra block indicate the both NNW and ENE lineaments, and there intersections points represent important locations to focus gold and base metal mineralization when hydrothermal fluids are present. This is used as a key vectoring criteria to carry out targeting on the entire Nitra block.

Two scales of target generation were completed including (i) a large-scale level of targeting integrating soil, lineament and available geophysical data on the eastern half of the Nitra block (**Fig. 22**) and (b) a coarse, small-scale level of targeting using lineament data, available geophysics and regional stream sediment geochemical data for the west Nitra block (**Fig. 23**). Note that one of the eastern targets that was identified due to an anomalous ENE lineament array also coincides with a prominent zone of magnetic destruction (**Fig. 24**).

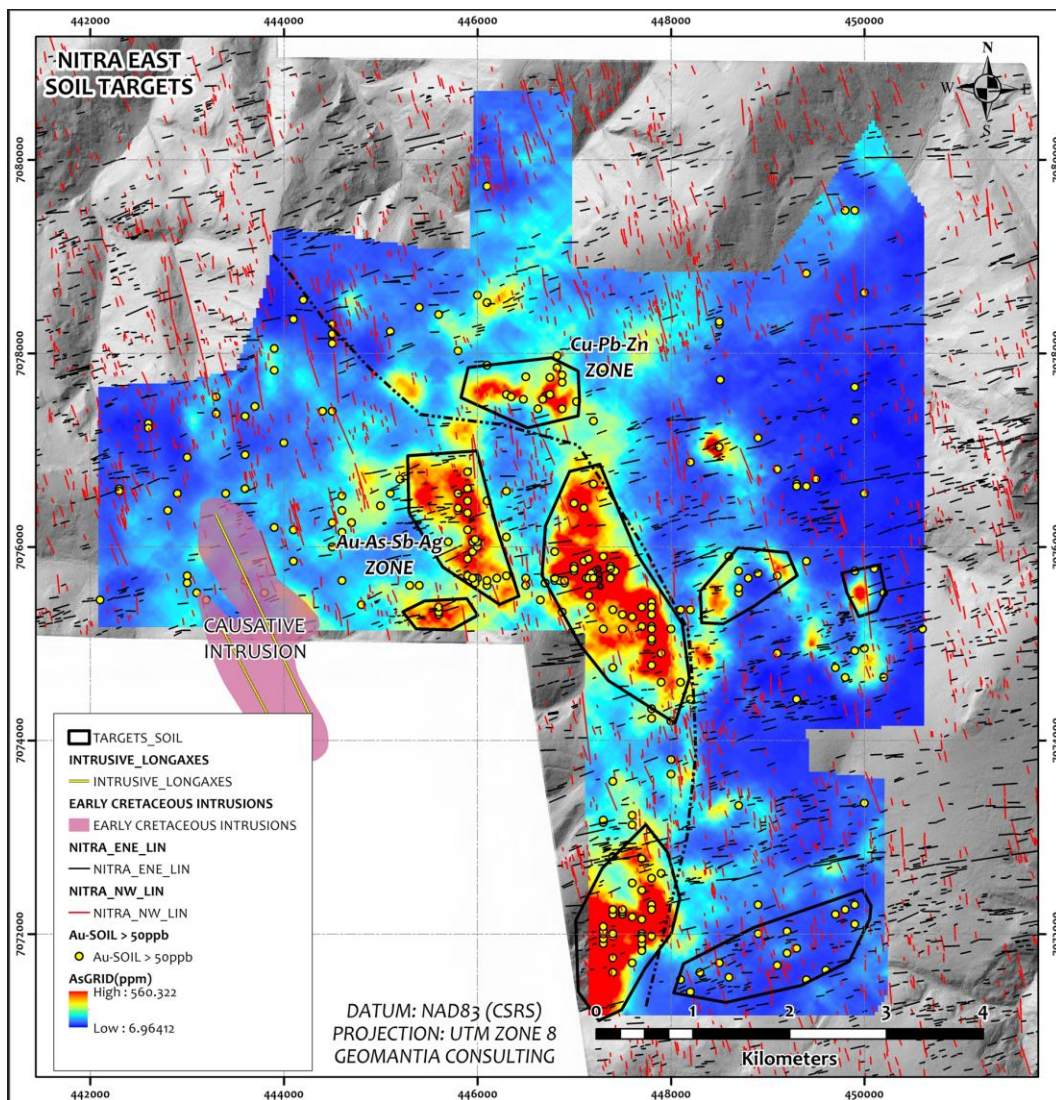


FIGURE 22: Eastern Nitra focused targets.

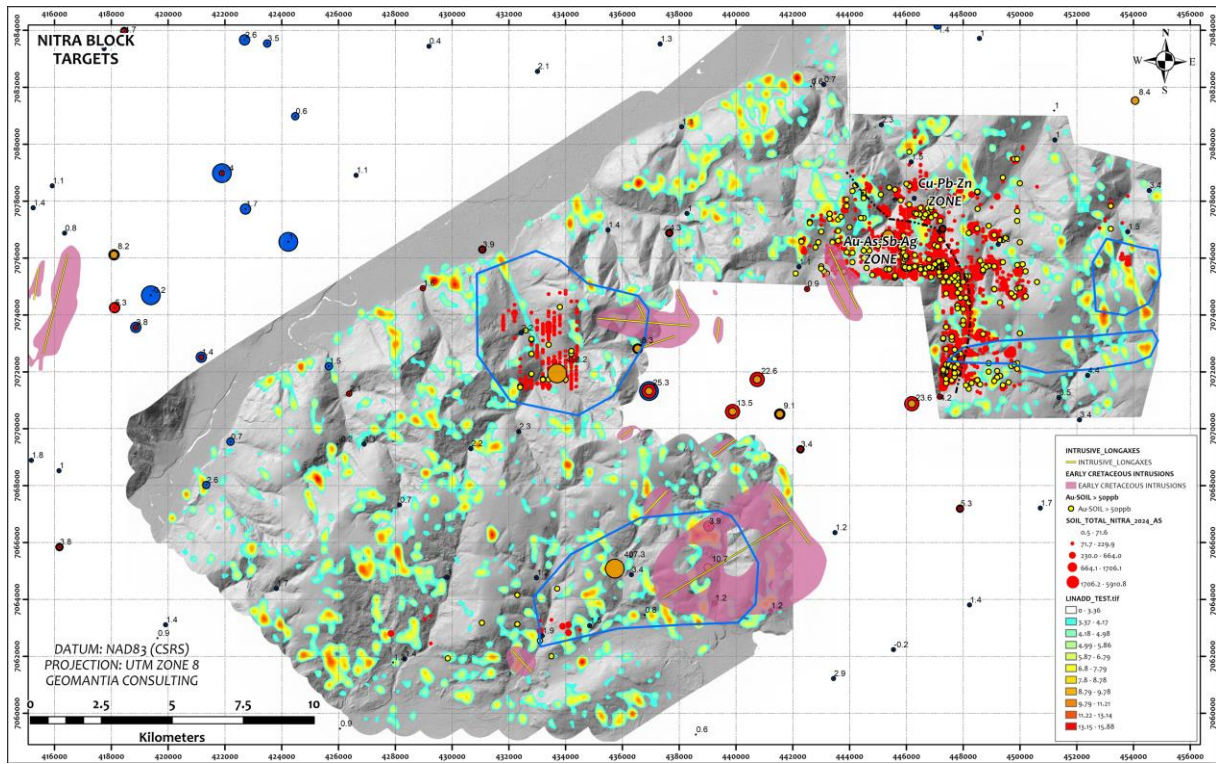


FIGURE 23: Block-scale target – Nitra project.

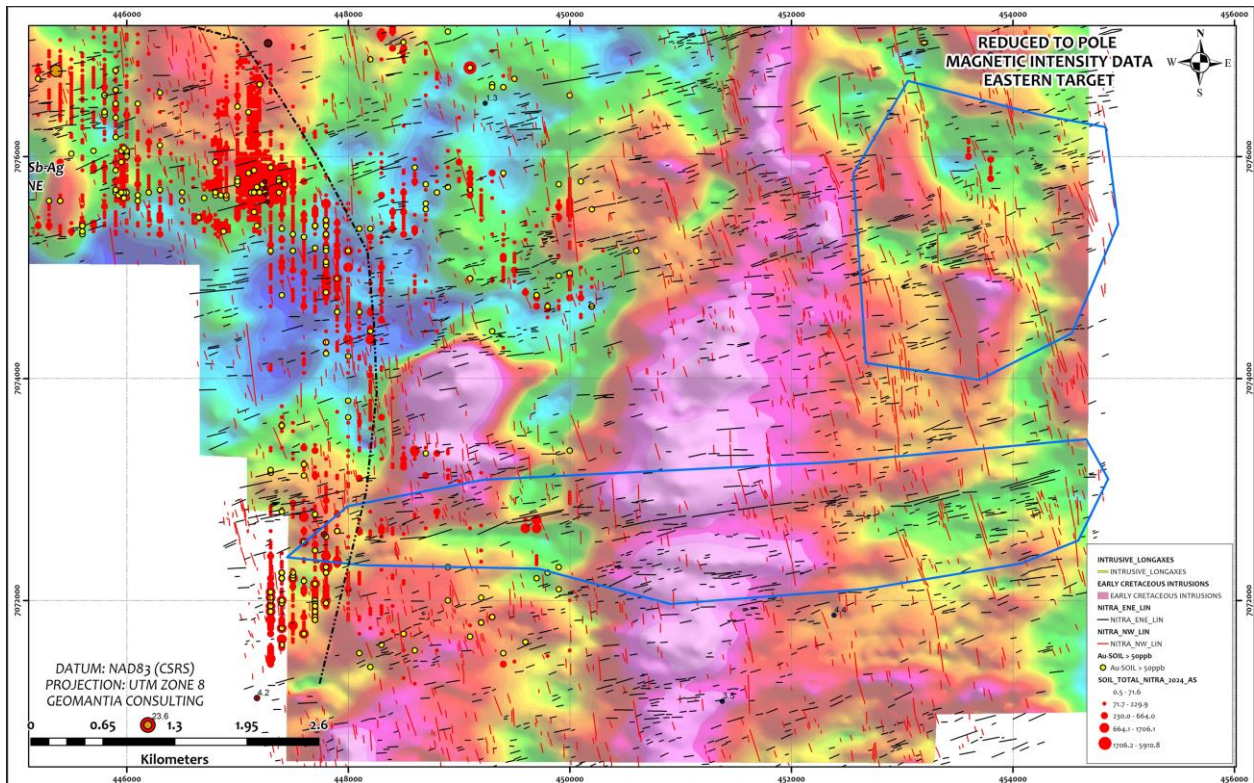


FIGURE 24: Eastern block-scale target and reduced to pole magnetic intensity data – Nitra project.

## **7.0 SUMMARY & RECOMMENDATIONS**

Airborne LiDAR survey data were acquired and reprocessed to conduct targeting over the Nitra block located approximately 30 km northwest of the village of Mayo and 100 % owned by Banyan Gold Corporation. The objective of the analysis was to better understand potential bedrock controls that may control gold mineralization in the area and use that understanding to generate targets for future exploration.

Raw Lidar data were acquired from McELhanney Ltd. and reprocessed to create a series of high resolution hillshade models that represent the ground surface without vegetation. Systematic 1:3 000 scale lineament mapping of the LiDAR data revealed the presence of three main lineament populations similar to the Aurmac project area. The eastern half of the Nitra block is characterized by a noticeable suite of NNW trending through-going linears and a subordinate set of ENE trending linears.

A review of soil geochemical data indicates that known zones of anomalism appear to be directly spatially associated with both these lineament populations and their intersections. Additionally, integration of soil geochemistry and lineament data for the eastern side of the Nitra block suggest metal suite zonation outboard (SW to NE) from a potential causative Tombstone age intrusion. Several small-scale and block-scale reconnaissance targets were generated from all available datasets.

Recommendations include:

1. Detailed prospecting in the eastern Nitra block in the target areas identified.
2. Mapping (as best as outcrop conditions allow) in western Nitra.
3. Trenching and/or drilling the eastern Nitra targets.
4. Silt geochemical program across western Nitra.
5. Expansion of radiometric/magnetic airborne survey to western Nitra.

## 8.0 STATEMENT OF QUALIFICATIONS

I, Venessa Bennett, P.Geo, with business and residential addresses in Whitehorse, Yukon Territory do hereby certify that:

1. I graduated from the Macquarie University, Sydney, Australia in 1996 with a B.Sc. (Hons) in geology, in 2008 from Memorial University of Newfoundland with a Ph.D. majoring in geology and in 2015 from the Centre of Geographic Sciences, Nova Scotia with an advanced diploma in Geographic Information Systems and Remote Sensing.
2. I am a Professional Geoscientist registered with the Association of Professional Engineers and Geoscientists of the Province of Alberta (**registration number - 192895**).
3. From 1996 to present, I have been actively engaged as a geologist in mineral exploration, geoscience research and government geoscience both internationally and nationally.
4. I personally completed the work reported herein and have interpreted all data resulting from this work.

Respectfully Submitted,

*Venessa Bennett*

---

Venessa Bennett Ph.D., P.Geo., Adv. Dip GIS/RS